ARTICLE IN PRESS

Available online at www.sciencedirect.com

SCIENCE DIRECT®

ELSEVIER

Applied Mathematical Modelling xxx (2005) xxx–xxx

APPLIED MATHEMATICAL MODELLING

www.elsevier.com/locate/apm

A comparison of adaptive time stepping methods for coupled flow and deformation modeling

Susan E. Minkoff [a,*], Nicholas M. Kridler [b]

[a] *Department of Mathematics and Statistics, University of Maryland, Baltimore County, 1000 Hilltop Circle, Baltimore, MD 21250, USA*
[b] *10833 Meadow Glen Way East, Escondido, CA 92026, USA*

Received 1 June 2004; received in revised form 1 July 2005; accepted 2 August 2005

Abstract

Many subsurface reservoirs compact or subside due to production-induced pressure changes. Numerical simulation of this compaction process is important for predicting and preventing well-failure in deforming hydrocarbon reservoirs. However, development of sophisticated numerical simulators for coupled fluid flow and mechanical deformation modeling requires a considerable manpower investment. This development time can be shortened by loosely coupling pre-existing flow and deformation codes via an interface. These codes have an additional advantage over fully-coupled simulators in that fewer flow and mechanics time steps need to be taken to achieve a desired solution accuracy. Specifically, the length of time before a mechanics step is taken can be adapted to the rate of change in output parameters (pressure or displacement) for the particular application problem being studied. Comparing two adaptive methods (the local error method—a variant of Runge–Kutta–Fehlberg for solving ode's—and the pore pressure method) to a constant step size scheme illustrates the considerable cost savings of adaptive time stepping for loose coupling. The methods are tested on a simple loosely-coupled simulator modeling single-phase flow and linear elastic deformation. For the Terzaghi consolidation problem, the local error method achieves similar accuracy to the constant step size solution with only one third as many mechanics solves. The pore pressure method is an inexpensive adaptive method whose behavior closely follows the physics of the problem. The local error method, while a more general technique and therefore more expensive per time step, is able to achieve excellent solution accuracy overall.

Keywords: Coupled processes; Adaptivity; Mechanics; Flow; Petroleum engineering

1. Introduction

When fluids such as oil and gas are extracted from subsurface reservoirs during production, pore pressure depletion may lead to compaction. In many cases, the compaction is small, but in well-known instances, this subsidence has caused well-failures, platform collapse, and even loss of human lives. The Ekofisk Field in the

* Corresponding author. Tel.: +1 410 455 3029; fax: +1 410 455 1066.
E-mail addresses: sminkoff@math.umbc.edu (S.E. Minkoff), nicholas.kridler@colorado.edu (N.M. Kridler).

0307-904X/$ - see front matter
doi:10.1016/j.apm.2005.08.002

North Sea [1,2] and Belridge in California [3] are dramatic examples where substantial subsidence led to major facilities damage.

In order to predict and hence prevent such catastrophic situations in the future, numerical simulation of these fields is important. Traditionally, flow simulators assume that only small deformations occur, and compaction is modeled by a rock compressibility term in the flow equations. Recently, it has become more common to model large-deformation reservoirs by coupling full-scale mechanical deformation codes with full-scale flow simulators. These coupled simulators are capable of modeling realistic physics which may include multiphase flow and nonlinear, inelastic deformation [4–6].

Coupled simulators fall into one of two main categories—full or loose coupling. Full coupling requires that one develop a single set of equations which connects flow to mechanics tightly (in other words, the flow equations contain terms for deformation and vice versa, see [7–11]). While these simulators are able to closely mimic the physics, they often require that modelers start from scratch to develop both the system of equations and the code to solve these equations. Development time and cost constraints often require the builders to simplify the flow and deformation models used in fully-coupled simulators. An attractive alternative to full coupling is to hook together two independent codes (flow and deformation) through an interface (loose coupling) [5]. Settari and Mourits [12] and Dean et al. [13] discuss iterative schemes which attempt to ensure the loosely-coupled solution converges to the fully-coupled (''true'') solution.

In this work we focus on adaptive time stepping schemes for a loosely-coupled, staggered-in-time flow and deformation simulator in which pressure changes are passed from flow to mechanics and changes in strain are sent from mechanics back to flow (for more details on the idea behind the coupling scheme, see [5]). We have chosen here to work with the simplest model (linear elasticity and single-phase flow) to isolate and illuminate the advantages and disadvantages of the different time stepping schemes themselves. Clearly more sophisticated models (plastic constitutive models, multiphase flow, etc.) are appropriate for modeling many realistic production scenarios involving compaction. However, this work is focused on the comparison of adaptive time stepping schemes for loosely coupled multiphysics simulations. These schemes are similar in nature to those investigated by Sinkin et al. [14] for optical fiber communication modeling. However, Sinkin applied adaptive time stepping methods to a single (not multi-) physics simulator. In this work, we assume the flow time step is fixed and adapt the size of the mechanics step. The cost saving in the loose coupling scheme comes from the fact that we need not solve the mechanics equations at each flow step (as with full coupling). Instead, multiple flow steps are taken, and when the accumulated change in pore pressure or displacement reaches a certain level, control is passed to the mechanical deformation code. The deformation code then solves the same set of time steps just solved by flow using flow input directly.

We test all of our time stepping schemes on a simple problem (the Terzaghi consolidation problem) which models compaction of a one-dimensional column of soil. A sudden load is applied to the top of the column at the start, and fluids drain from the surface causing pressure to decrease and compaction to occur.

The remainder of this paper describes the physical flow and deformation models and the discretization and solution of these governing equations using the finite element method. The three time stepping schemes (constant step size, pore pressure, and local error method) are then described in detail. Finally, we compare the results of running these schemes on the model Terzaghi consolidation problem. The solutions compare favorably in terms of accuracy, and we see that there is a substantial saving in number of mechanics steps taken with adaptive time stepping over fixed step size.

2. Mathematical models

Because our focus in this study is on comparison and analysis of different adaptive time stepping techniques for loose coupling, we chose to use simple flow and deformation models as inputs to the scheme. The fluid flow model is single-phase flow in one-dimension. For mechanics we assume a linearly elastic model. (More sophisticated physical models are described in the context of coupled simulations in [5,6].) Both the single-phase flow and linear elasticity models are described below.

2.1. Fluid flow

An important component of fluid flow modeling is Darcy's Law which relates the fluid velocity, u, to the gradient of the pore pressure, p, for a porous medium. The rate of flow is inversely proportional to the fluid viscosity, μ. Darcy's Law says that

$$u = \frac{Q}{A} = -\frac{k}{\mu}(\nabla p - \rho g \nabla Z). \tag{1}$$

Here Q is the rate of flow, A the cross-sectional area, and k is the permeability of the medium. Depth is denoted by Z, gravity by g, and ρ is fluid density. Darcy's Law combined with conservation of mass produces the equation governing single-phase flow through a porous medium:

$$\frac{\partial(\phi\rho)}{\partial t} = \nabla \cdot \left(\frac{k\rho}{\mu}(\nabla p - \rho g \nabla Z)\right) + q. \tag{2}$$

In this equation, ϕ is porosity and q is the source. Physically, q will model an injection or production well. (The description of the flow equations in this paper closely follows the derivation given in [15].) For the problem presented in this paper, we neglect gravity. In essence, the compaction caused by coupling to mechanical deformation will account for the effect of gravity.

Eq. (2) involves two unknowns: pressure and density. To solve this equation uniquely for one of the two unknowns, we add the fluid compressibility constraint ([15] and references therein) which relates pressure and density:

$$c = \frac{1}{\rho}\frac{\partial \rho}{\partial p}. \tag{3}$$

This first-order ordinary differential equation (ode) can be solved via separation of variables to give density in terms of pressure:

$$\rho = \rho_0 e^{c(p-p_0)}, \tag{4}$$

where p_0 is the initial pressure and ρ_0 is the initial density. Rewriting Eq. (4) in terms of pressure we arrive at:

$$p = p_0 + \frac{1}{c}\log\frac{\rho}{\rho_0}. \tag{5}$$

Eq. (3) allows us to rewrite Eq. (2) for the single variable density

$$\frac{\partial(\phi\rho)}{\partial t} = \nabla \cdot \left(\frac{k}{\mu c}\nabla\rho\right) + q \tag{6}$$

or as an equation just for pressure,

$$\frac{\partial(\phi\rho_0 e^{c(p-p_0)})}{\partial t} = \nabla \cdot \left(\frac{k}{\mu c}\nabla p\right) + q. \tag{7}$$

Because the pressure equation is nonlinear, we initially attempted to solve Eq. (6) for density (and then post-processed for pressure). Unfortunately, the boundary conditions are more naturally posed in terms of pressure, and hence our solution was difficult to validate against standard solutions. For this reason, we chose instead to solve a linearized version of the pressure equation (7). Assuming fluid compressibility is small, we can approximate density ρ in Eq. (4) by the truncated Taylor series,

$$\rho = \rho_0(1 + c(p - p_0)). \tag{8}$$

The linearized version of Eq. (7) is then given by

$$\rho_0\frac{\partial(\phi p)}{\partial t} = \nabla \cdot \left(\frac{k}{\mu c}\nabla p\right) + q. \tag{9}$$

We will focus on the one-dimensional case without an external source term. (For the problem discussed in this paper, the source of compaction and fluid drainage comes from the initial conditions rather than an external source. See Section 4.) Thus the final version of the flow equation which we solve in our coupled system is

$$\rho_0 \frac{\partial(\phi p)}{\partial t}(x,t) = \frac{k}{\mu c}\frac{\partial^2 p}{\partial x^2}(x,t). \tag{10}$$

2.2. Mechanical deformation

We will assume linear elasticity for deformation [16]. If f is the external load and σ the stress, we attempt to equilibrate the change in stress against body forces:

$$-\frac{\mathrm{d}\sigma}{\mathrm{d}x} = f. \tag{11}$$

The constitutive law relating stress to strain in this case is Hooke's Law:

$$\sigma = \lambda \frac{\mathrm{d}u}{\mathrm{d}x} + \hat{\mu}\varepsilon(u), \tag{12}$$

where u is the displacement, λ and $\hat{\mu}$ are the Lamé constants of elasticity, and the one-dimensional strain ε is defined as the derivative of displacement:

$$\varepsilon(u) = \frac{\mathrm{d}u}{\mathrm{d}x}. \tag{13}$$

Combining Eqs. (11)–(13) results in the second-order differential equation for displacement in 1-D:

$$-(\lambda + \hat{\mu})\frac{\mathrm{d}^2 u}{\mathrm{d}x^2} = f. \tag{14}$$

2.3. Coupled flow and deformation

To loosely couple these two models, we will consider the change in pore pressure to be an external force for mechanics. Thus we augment the right hand side of Eq. (14).

$$-(\lambda + \hat{\mu})\frac{\mathrm{d}^2 u}{\mathrm{d}x^2} = f - \frac{\mathrm{d}p}{\mathrm{d}x}. \tag{15}$$

The resulting volume strain ε, calculated from solving Eq. (15) and then post-processing via Eq. (13), is then used to update porosity for the next set of flow time steps (see Fig. 1). The porosity update formula is:

$$\phi(x,t) = 1 - \frac{(1-\phi_0)}{e^{\varepsilon}}, \tag{16}$$

with ϕ_0 the initial porosity.

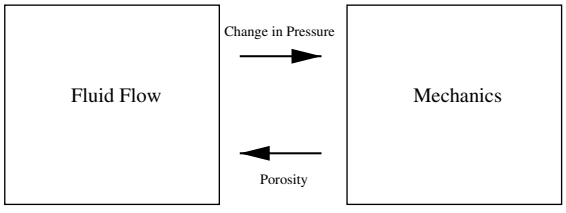

Fig. 1. Loose coupling of fluid flow and mechanics.

3. Numerical algorithm

For simplicity, we used the Galerkin finite element method to numerically discretize and solve the mathematical models described in the previous section. In this section we present the finite element variational formulation for both flow and mechanics. Given a domain $\Omega \in \Re$ for x, we define the space $U_N \in H_0^1(\Omega)$ to be the set of functions $\{u : u \in L^2(\Omega),\ \mathrm{d}u/\mathrm{d}x \in L^2(\Omega),\ u|_{\partial\Omega} = 0\}$. Piecewise linear ("hat") basis functions of the form $(\alpha x + \beta)$ represent the solution unknowns in our model equations (pressure for flow and displacement for mechanics).

3.1. Mechanics

If we multiply Eq. (15) by the test function, $v \in U_N$, and integrate over the domain Ω, the integral form of the equation becomes:

$$-\int_\Omega (\lambda + \hat{\mu}) \frac{\mathrm{d}^2 u}{\mathrm{d}x^2} v(x)\mathrm{d}x = \int_\Omega \left(f - \frac{\mathrm{d}p}{\mathrm{d}x}\right) v(x)\mathrm{d}x \quad \forall v \in V_N. \tag{17}$$

The test space is chosen to have compact support, so integration by parts applied to the left hand side of Eq. (17) results in the weak form of Eq. (15).

$$\int_\Omega (\lambda + \hat{\mu}) \frac{\mathrm{d}u}{\mathrm{d}x} \frac{\mathrm{d}v}{\mathrm{d}x}\mathrm{d}x = \int_\Omega \left(f - \frac{\mathrm{d}p}{\mathrm{d}x}\right) v(x)\mathrm{d}x \quad \forall v \in V_N. \tag{18}$$

We will look for a finite dimensional solution u_h which we write as a linear combination of basis functions ψ_j:

$$u_h(x) = \sum_{j=1}^{N} \xi_j \psi_j(x). \tag{19}$$

Substituting this sum into Eq. (18) and choosing test functions from the same space, we arrive at the system of equations:

$$\sum_{j=1}^{N} \xi_j \int_\Omega (\lambda + \hat{\mu}) \frac{\mathrm{d}\psi_j}{\mathrm{d}x}(x) \frac{\mathrm{d}\psi_i}{\mathrm{d}x}(x)\mathrm{d}x = \int_\Omega \left(f - \frac{\mathrm{d}p}{\mathrm{d}x}\right) \psi_i(x)\mathrm{d}x \tag{20}$$

for $i = 1, \ldots, N$. Defining the stiffness matrix K and load vector f to be:

$$K_{ij} = \int_\Omega (\lambda + \hat{\mu}) \frac{\mathrm{d}\psi_j}{\mathrm{d}x}(x) \frac{\mathrm{d}\psi_i}{\mathrm{d}x}(x)\mathrm{d}x, \tag{21}$$

$$f_i = \int_\Omega \left(f - \frac{\mathrm{d}p}{\mathrm{d}x}\right) \psi_i(x)\mathrm{d}x, \tag{22}$$

we wish to solve the matrix system:

$$K\xi = f. \tag{23}$$

3.2. Fluid flow

Multiplying Eq. (10) by a test function and integrating over the domain Ω gives:

$$\int_\Omega \rho_0 \frac{\partial(\phi p)}{\partial t} v(x)\mathrm{d}x = \int_\Omega \frac{k}{\mu c} \frac{\partial^2 p}{\partial x^2} v(x)\mathrm{d}x \quad \forall v \in V_N. \tag{24}$$

We then apply integration by parts to the spatial derivative on the right and note that the boundary term again vanishes due to the choice of test space. Eq. (24), therefore, becomes

$$\int_\Omega \rho_0 \frac{\partial(\phi p)}{\partial t} v(x)\mathrm{d}x = -\int_\Omega \frac{k}{\mu c} \frac{\partial p}{\partial x} \frac{\partial v}{\partial x}\mathrm{d}x \quad \forall v \in V_N. \tag{25}$$

Finally, we search for a pressure solution in a finite dimensional subspace of dimension N,

$$p_h(x) = \sum_{j=1}^{N} \xi_j(t)\psi_j(x), \tag{26}$$

with $\{\psi_j\}_{j=1}^{N}$ forming a basis for V_N. The fluid flow equation is solved via the discrete system of equations,

$$\sum_{j=1}^{N} \frac{\mathrm{d}\xi_j}{\mathrm{d}t}(t) \int_\Omega \rho_0 \phi(x)\psi_j(x)\psi_i(x)\mathrm{d}x = -\sum_{j=1}^{N} \xi_j(t) \int_\Omega \frac{k}{\mu c} \frac{\mathrm{d}\psi_j}{\mathrm{d}x}(x) \frac{\mathrm{d}\psi_i}{\mathrm{d}x}(x)\mathrm{d}x, \tag{27}$$

with $i = 1, 2, \ldots, N$. In this equation, porosity depends only on the spatial variable x. When compaction occurs, however, porosity changes. Thus there is a loose dependence of porosity on time through mechanics.

Defining the mass matrix M and stiffness matrix K by

$$M_{ij} = \int_\Omega \rho_0 \phi(x)\psi_j(x)\psi_i(x)\mathrm{d}x, \quad \text{and} \quad K_{ij} = \int_\Omega \frac{k}{\mu c} \frac{\mathrm{d}\psi_j}{\mathrm{d}x}(x) \frac{\mathrm{d}\psi_i}{\mathrm{d}x}(x)\mathrm{d}x, \tag{28}$$

we can reduce the flow equation to a system of ordinary differential equations

$$M\frac{\mathrm{d}\xi}{\mathrm{d}t}(t) + K\xi(t) = 0. \tag{29}$$

We employ a backward Euler scheme [17] to solve Eq. (29) numerically. These schemes are appropriate for CFL-restricted parabolic equations. This method produces a solution at the n-th time step via the iteration:

$$(M + \Delta t K)\xi^{(n+1)} = M\xi^n. \tag{30}$$

3.3. Adaptive time stepping

We compare three techniques for adaptive time stepping in loose coupling of flow and deformation: the local error method, the pore pressure method, and constant step size. Adaptivity in our context means adapting the length of the *mechanics* step. It is assumed that the changes in fluid flow parameters (pressure) will occur on a shorter time scale than changes in mechanics (displacement). While this assumption will not always hold, pressure changes are often the limiting factor in the growth of time step size for realistic coupled simulation [5]. Thus we fix the flow time (in the examples described here, for example, at .001 s) and mechanics steps are taken after a set of flow time steps are completed. Initially the mechanics steps might be taken every .01 s (i.e., every 10 flow steps). As the simulation progresses, the mechanics time step size will change to accommodate the physics of the problem. (For the problem described in this paper, the most dramatic pressure changes occur at the start of the experiment. After this initialization stage, the mechanics step begins to grow.)

The constant step size method fixes the mechanics step size throughout the coupled simulation. This technique is the simplest and most common for loose coupling. It does not involve adaptivity. We use the constant step size solution (with very small mechanics steps) as our benchmark "true solution" against which we compare the local error and pore pressure adaptive solutions. Our ultimate goal is to compare numerical solutions for accuracy and cost. The constant step size method is the most expensive in terms of total number of mechanics time steps taken.

The local error method (or adaptive Runge–Kutta–Fehlberg technique) was developed for adaptively solving ode's numerically [18,19]. It is easy to implement, and the structure of the algorithm does not depend on the particular problem being solved. (See the paper by Sinkin et al. [14] for use of this method in a fiber optics simulator.) With the local error method, we seek the best (i.e., the largest) mechanics time step given a prescribed bound on the maximum error allowable for a particular simulation output quantity. We chose to define this bound or "goal local error", δ_g, in terms of the change in displacement. The method starts with an initial step size t and a specified goal local error. We run the fluid flow simulation for a total time of $2t$. We then solve the mechanics equations for the same total length of time ($2t$). The resulting solution is called the coarse displacement solution, u_c. For comparison, we then rerun the same mechanics simulation, solving the

mechanics equations in two steps each of length t. We call this solution the fine displacement solution u_f. By looking at the relative error between these two solutions, we can determine whether the larger time step is acceptable or whether it incurs too great of a change in displacement ("error") for one time step.

The simulation error defined by

$$\delta = \frac{\|u_f - u_c\|_2}{\|u_f\|_2}. \tag{31}$$

is compared to the goal local error δ_g. We determine whether to keep or reject the time step size via the following algorithm:

3.3.1. Algorithm

if $\delta < \frac{1}{2}\delta_g$,
    Accept current solution, and increase the size of the next mechanics step.
else if $\delta \in (\frac{1}{2}\delta_g, \delta_g)$,
    Accept current solution, and hold the step size fixed for the next mechanics step.
else if $\delta \in (\delta_g, 2\delta_g)$,
    Accept current solution, but decrease the size of the next mechanics step.
else if $\delta > 2\delta_g$,
    Throw current results away, cut the step size in half, and retry.

The third method we looked at was the pore pressure method. This algorithm is a simple adaptive scheme in which the output from the flow simulator determines when to pass control to mechanics. The algorithm requires that we again specify a tolerance (this time on the magnitude of the change in pore pressure). The flow simulator runs until the quantity $\frac{1}{\Delta p} <$ tol where Δp is the change in pore pressure. When Δp becomes larger than our tolerance allows, control is sent to mechanics. Since the deformation code uses the change in pore pressure to augment the load vector, too great a change will result in a load vector that mechanics will have difficulty matching to changes in displacement. Thus, the change in pore pressure is a reasonable quantity to assess before making the decision to continue with flow simulation or switch to deformation.

In both the local error and pore pressure methods, the choice of tolerances can be difficult to determine a priori. The pore pressure tolerance has a much clearer physical meaning than the goal local error tolerance, but still trial and error and an understanding of the physical behavior of the particular problem are required.

4. Numerical results

4.1. Terzaghi consolidation problem

Our comparisons of the three time stepping schemes are all based on the Terzaghi consolidation problem—a classic one-dimensional test problem [20]. For this model problem, we consider a thin body of soil, i.e. a column of mud which is 100 inches high, confined by smooth, impermeable, rigid walls on all sides except the top surface (see Fig. 2). On the surface, perfect drainage is possible, and a load is applied suddenly to the column. Drainage is modeled by a zero Dirichlet condition at the top. In all of the experiments we describe, the one-dimensional column is discretized using approximately 30–60 grid points in z. Numerical simulation will allow us to predict the evolution of displacement, effective stress, and pore pressure throughout the column as a function of time following the application of the load.

The specific inputs to the Terzaghi consolidation problem that we discuss in this paper were based on the ABAQUS test problem for one-dimensional consolidation [21] Section 3.1.5. In particular, the column of mud is assumed to be linearly elastic with a Young's modulus of $E = 10^8$ lb/in.^{2}, Poisson's ratio of $v = 0.3$, an initial porosity $\phi_0 = 0.6$ (derived from a void ratio of 1.5), and permeability, $k = 1.86 \times 10^{-11}$ in/s. The fluid compressibility is 1.2×10^{-8} psi, viscosity $\mu = 5.6 \times 10^{-5}$ psi-s, and the initial pressure is taken to be $p_0 = 10^8$ psi.

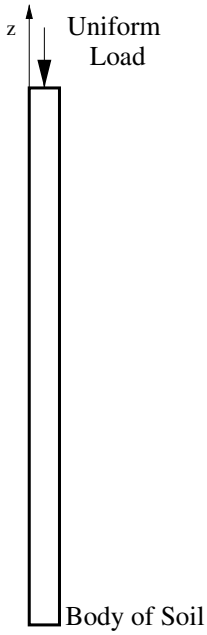

Fig. 2. Model for Terzaghi consolidation problem.

The Terzaghi consolidation problem permits an analytic solution for pressure which results from Laplace transforming the consolidation equation [20]. This solution is given by the following power series ([22–24] and references therein):

$$\frac{p}{p_0} = \sum_{m=0}^{\infty} \left(\frac{2}{M}\right) \sin\left(\frac{Mz}{h}\right) \exp\left(-2M^2 T_v\right). \tag{32}$$

In formula (32) pressure has been normalized by the initial pressure p_0 and $M = (2m+1)\pi/2$. Other inputs to this equation include h which is the original height of the column of mud, z which is the depth of interest within the column, and a dimensionless time factor of the form $T_v = c_v t/h^2$. This time factor includes physical time t, and the consolidation coefficient [20,23,24] defined by

$$c_v = \frac{\kappa}{(m_v + \phi c)\gamma_w}. \tag{33}$$

In the formula above, κ is hydraulic conductivity, c is fluid compressibility, γ_w is the volumetric weight of water (taken here to be 1 lb/in.^{3}), and m_v is the compressibility coefficient [23,24] defined in terms of stress, strain, and pressure as

$$m_v = -\varepsilon/(\sigma - p). \tag{34}$$

Further details and comparisons for this basic problem may be found in [25,22,26,27,21,23,24].

Figs. 3–5 give comparisons between the analytic solution (curve marked by asterisks) and the numerical solution from our coupled code (thin solid line) at three different heights in the column of mud. Fig. 3 shows the validation towards the top of the 100 in. column (80 in. from the ground) where changes in column height, stress, and pore pressure are greatest. Agreement is good if not exact. The differences seen in this figure are most likely due to one of the following assumptions in our simple model: the loose staggered-in-time coupling scheme, the fact that permeability is assumed constant in this work, or most likely, the fact that our rather large load does not satisfy the small-strain assumption required by Terzaghi's analytic solution. Figs. 4 and 5 show the validation at heights of 50 in. (the midpoint of the column) and 20 in. (near the bottom of the column of mud). Here the agreement between analytic and numerical solutions is excellent. While we agree that more sophisticated models would allow for more realistic modeling [5,6], for purposes of comparing adaptive time stepping schemes this agreement appears quite satisfactory.

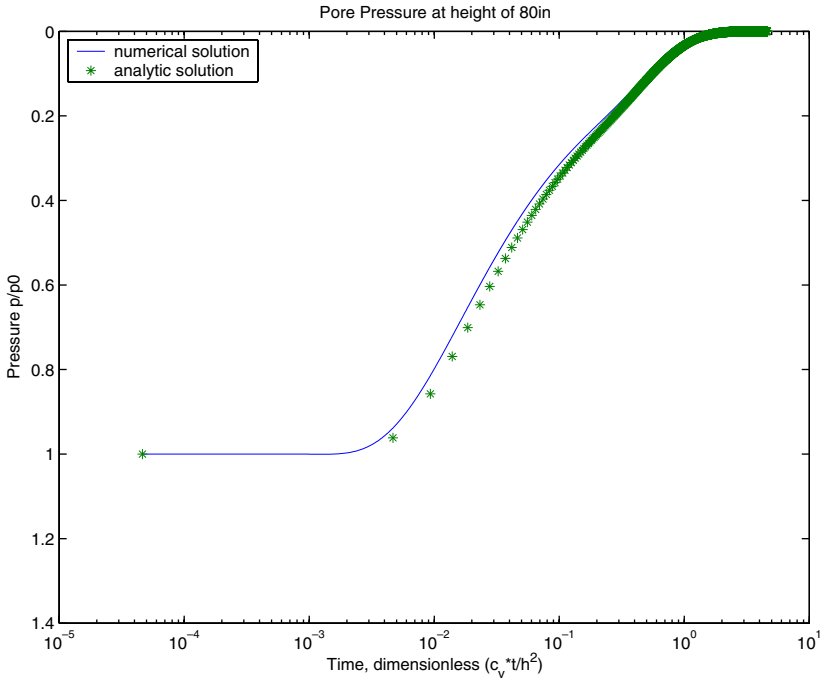

Fig. 3. Comparison of normalized pore pressure versus non-dimensional time ($c_v t/h^2$) for the Terzaghi consolidation problem at a height of 20 in. from the top of the 100-in. column. The curve denoted by asterisks is a plot of the analytic power series solution for the consolidation equation. The thin solid line is a plot of the numerical solution from the loose-coupling algorithm with constant step size.

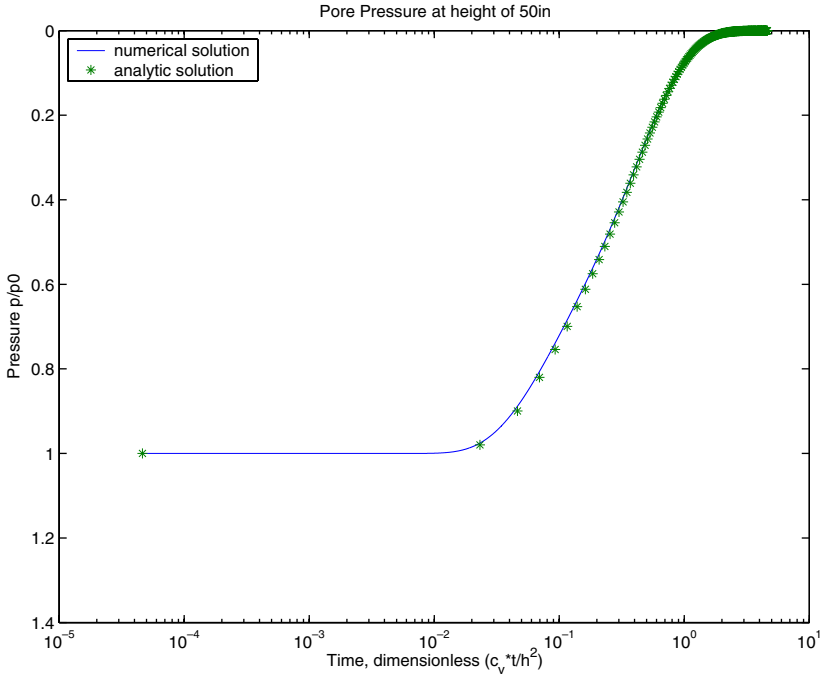

Fig. 4. Comparison of normalized pore pressure versus non-dimensional time ($c_v t/h^2$) for the Terzaghi consolidation problem at a height of 50 in. from the bottom of the 100-in. column. The curve denoted by asterisks is a plot of the analytic power series solution for the consolidation equation. The thin solid line is a plot of the numerical solution from the loose-coupling algorithm with constant step size.

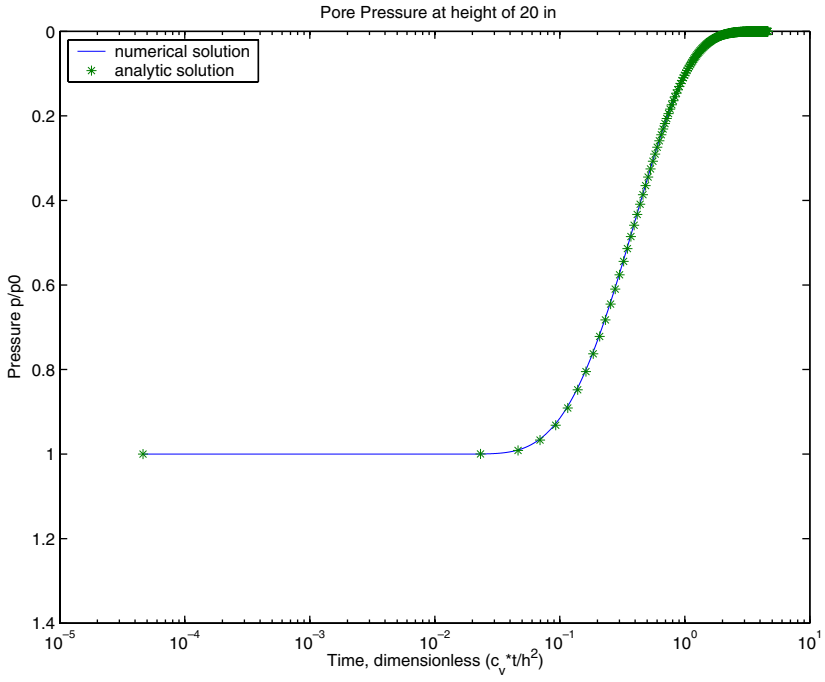

Fig. 5. Comparison of normalized pore pressure versus non-dimensional time ($c_v t/h^2$) for the Terzaghi consolidation problem at a height of 20 in. from the bottom of the 100-in. column. The curve denoted by asterisks is a plot of the analytic power series solution for the consolidation equation. The thin solid line is a plot of the numerical solution from the loose-coupling algorithm with constant step size.

4.2. Constant step size results

We now turn to the main purpose of this paper—comparison of numerical solutions coming from different time stepping schemes. We will use a constant step size solution run with small time steps as our benchmark for comparison. This choice is justified based on the validation experiment described in the preceding section. Time steps for the constant step size flow and deformation calculations were .001 s and .01 s, respectively. Fluids drain out of the top of the column of mud, so we expect to see a reduction in pore pressure as time progresses. Fig. 6 displays normalized pressure along the column at three different times during the simulation. The sudden application of the load causes a rapid change in pressure at the start of the simulation. With time, the change in pressure which has accumulated at the top of the column spreads down the length of the column.

Fluid drainage causes compaction and hence a substantial decrease in the height of this 100 in. column over time. Fig. 7 shows the evolution of displacement over 27.72 s. After 0.6 s, the column has compacted about 10 in. At the end of the numerical simulation, the column is less than half its original height. The normalized time evolution of stress and pore pressure at the point in the column corresponding to height 75 in. is shown in Fig. 8. As one would expect, stress and pressure are inversely correlated. As further validation of our numerical solution, we note that the curves in Figs. 6–8 all show good qualitative agreement with the solution found in [21, Section 3.1.5.].

4.3. Adaptive time stepping results

From Figs. 6 and 7, we see that there is a rapid decrease in both the pore pressures and displacements at the start of the simulation. For this reason we would expect our adaptive schemes will require small time steps initially. As time increases and the effect of the load has dispersed throughout the column, the time step size should increase. Fig. 9 shows the time step sizes for a 30 s simulation using the local error method and a goal local error tolerance of 10^{-4}. Recall that the goal local error tolerance is based on changes in displacement

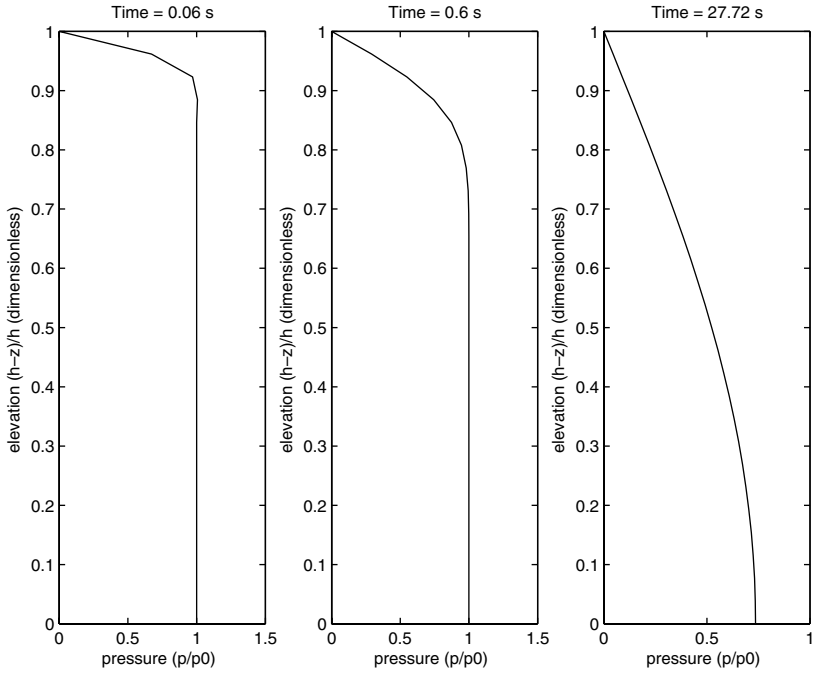

Fig. 6. Normalized pore pressure up to 27.72 s. The normalized column height ranges from "1" (top) to "0" (bottom). Notice the rapid decrease in pressure as soon as the load is applied.

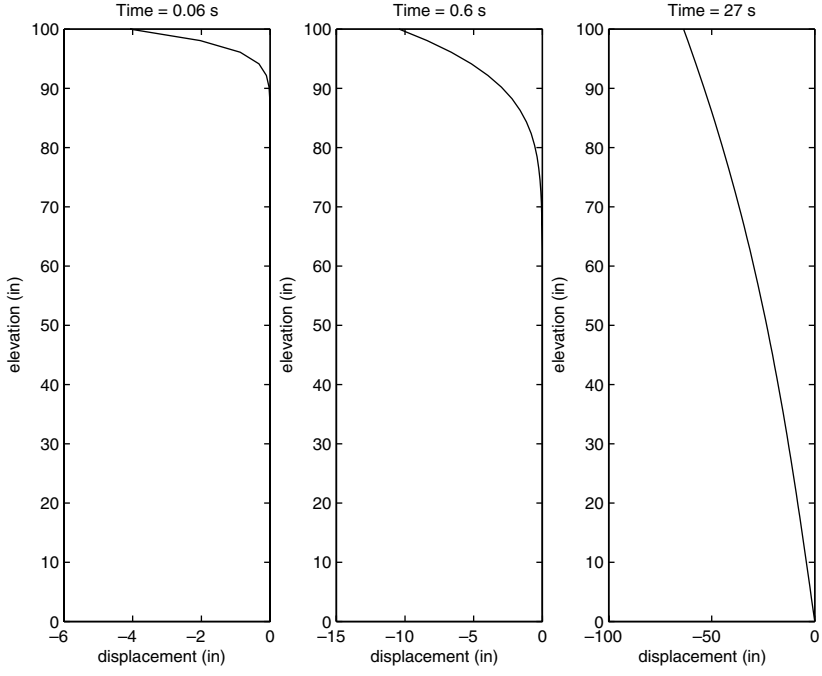

Fig. 7. Displacements up to 27.72 s. The negative numbers indicate the compaction of the column.

with time. Over the course of the 30 s simulation, we take just over 800 mechanics time steps which range in size from 10^{-4} s at the start of simulation to greater than 1 s towards the end. The local error method uses a quantized formula for calculating the size of the step for mechanics (see Algorithm 3.3.1). The parameters in

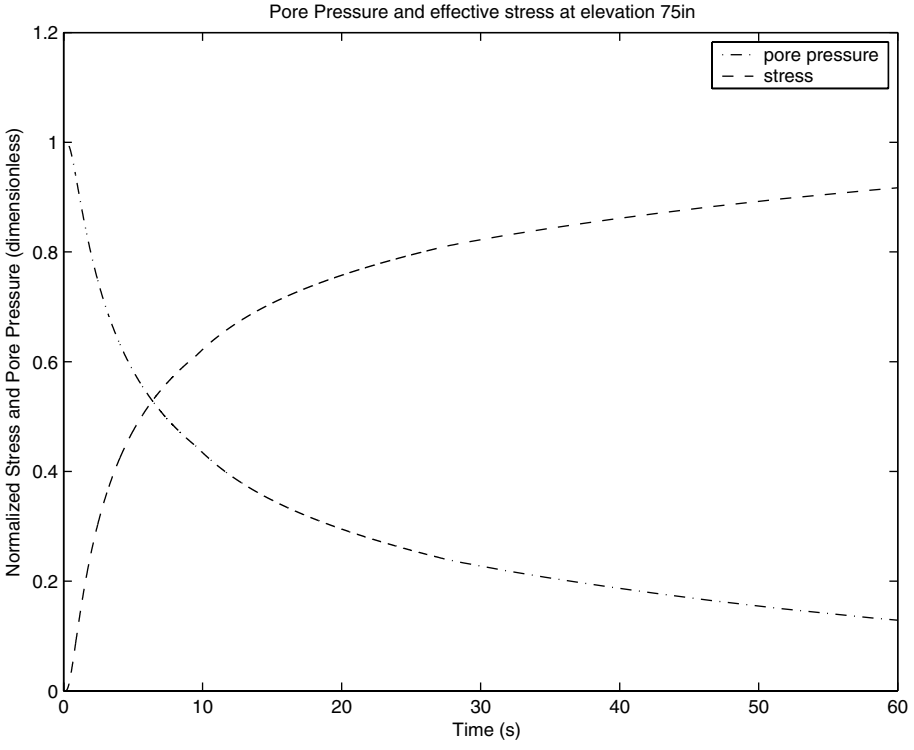

Fig. 8. Normalized pore pressure and stress at 75 in. from a 60 s simulation of the consolidation problem.

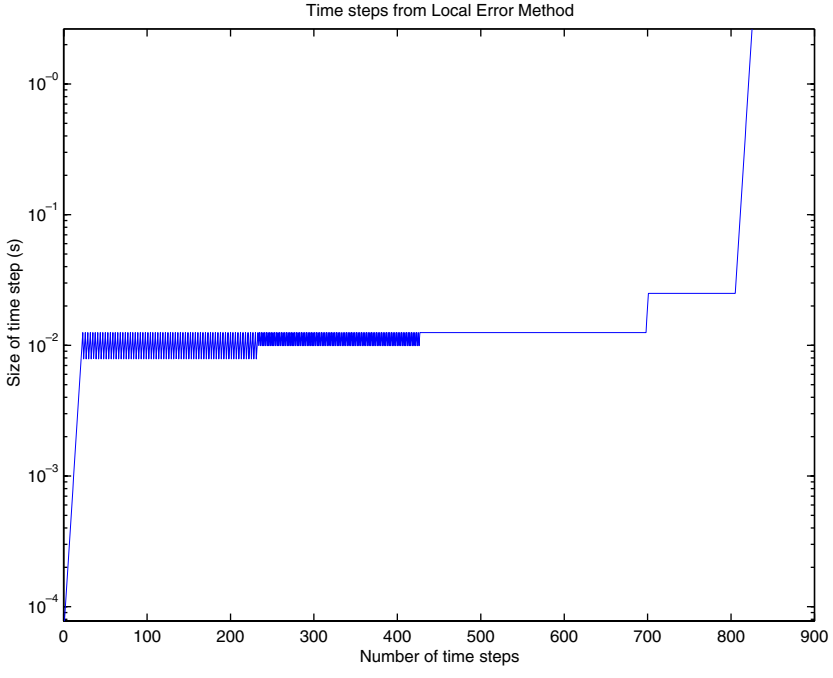

Fig. 9. Size of time steps taken over a 30 s simulation (using the local error method) with a goal local error of $\delta_g = 10^{-4}$.

the algorithm could be tuned to a particular problem. For example, the algorithm must choose a rule for decreasing or increasing subsequent time steps. We cut the time step in half if the error is greater than twice

the goal local error. One could instead choose to cut the step size by one-quarter or two-thirds, etc. Whatever the rule for modifying time step size, the local error method constructs buckets into which the results fall at each time step. This quantization can lead to a "chattering" effect as seen in Fig. 9 between time steps 0 and 400. The algorithm overshoots by choosing too large of a time step then corrects itself through time step reduction. However, the reduced time step is smaller than absolutely necessary and the cycle repeats. With the local error method, the choices for the size of the time step are limited.

Despite this step size quantization, the local error method appears to be accurate, as seen in Fig. 10. In this graph we see the displacement after 30 s from the adaptive time stepping algorithm compared to the solution calculated using small constant steps of size .005 s for mechanics. Moreover, running the constant step simulation required 6000 mechanics solves. The local error method with goal local error tolerance of 5×10^{-4} took only 2000 steps for the same total simulation time. (Note that Figs. 10 and 11 correspond to the same experiment as shown in Fig. 9 but with a smaller initial mechanics step size, hence more time steps are taken over the course of the 30 s simulation.) While this does not imply that the local error method is faster in wall-clock time, it does demonstrate that one can obtain computational savings from an adaptive scheme. Finally, Fig. 11 demonstrates the effect of the goal local error on the number of steps required. As expected, as we tighten the goal local error tolerance, the algorithm must take more time steps.

In Figs. 12–14 we illustrate the behavior of each of the three time stepping schemes: constant step size, pore pressure, and local error method for a suite of experiments parametrized by step size tolerance. Each figure is a graph of global relative error versus number of time steps. For example, the pore pressure method plot (Fig. 13) shows the result of running 18 experiments with tolerances ranging from 10^{-7} to 10^{-1}. The global relative error in all graphs is calculated by looking at the relative norm difference between the displacement for the adaptive scheme and the displacement coming from the constant step size method with mechanics steps of size 10^{-7}. Note that the flow time step is not adapted in these runs and hence can limit the error reduction in some cases. (The mechanics steps cannot fall below the size of the pressure steps.)

Figs. 12 and 13 indicate that the constant step size and pore pressure methods behave similarly for the suite of experiments. This similarity is to be expected as the pore pressure method is a very simple adaptive scheme

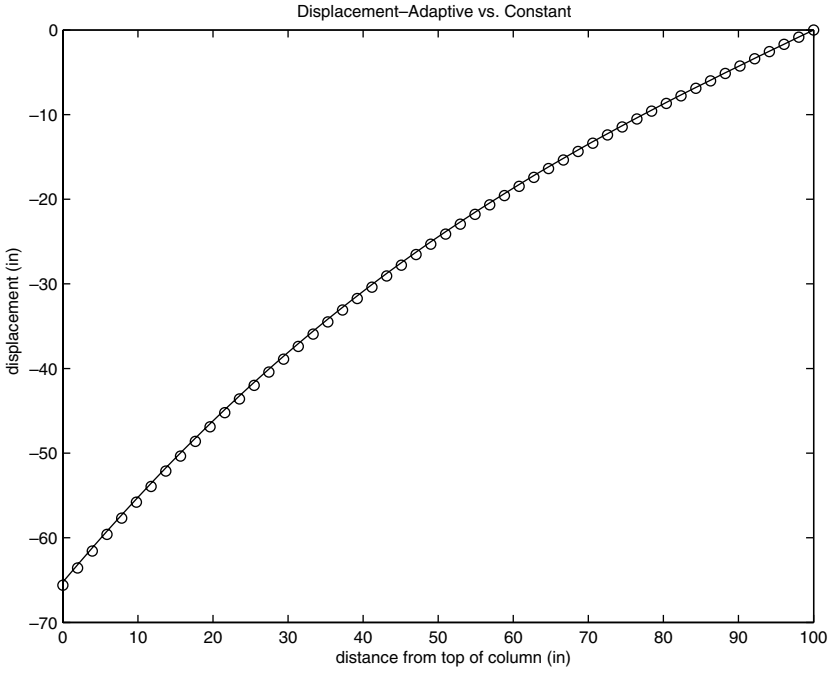

Fig. 10. Results of the local error method: displacement vs. column height after 30 s using a goal local error of $\delta_g = 5e-4$. The constant step-size solution is given by the solid line. The local error method solution is denoted by circles.

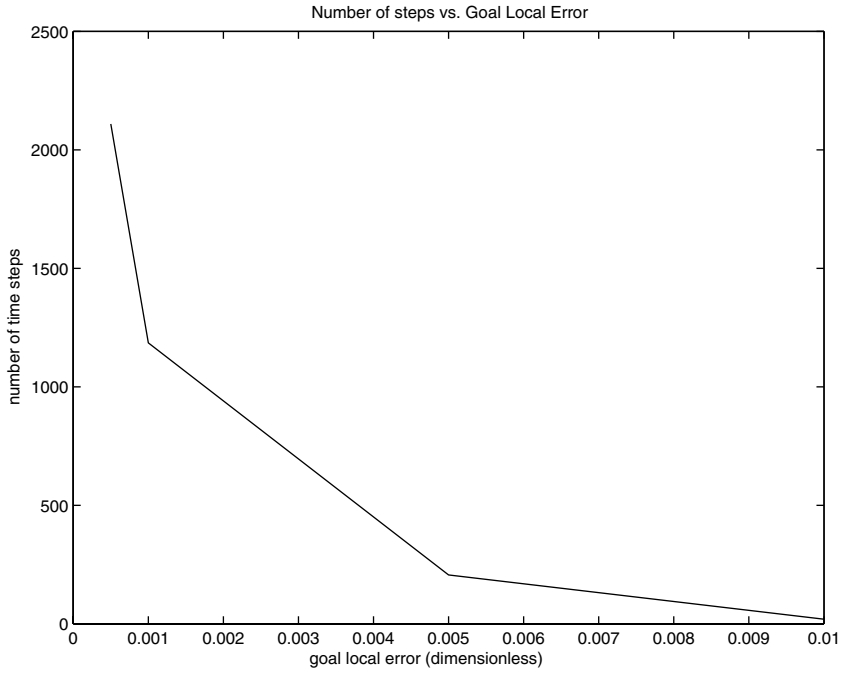

Fig. 11. The number of mechanics steps required to complete a 30 s simulation using the local error method and different goal local errors for adaptivity.

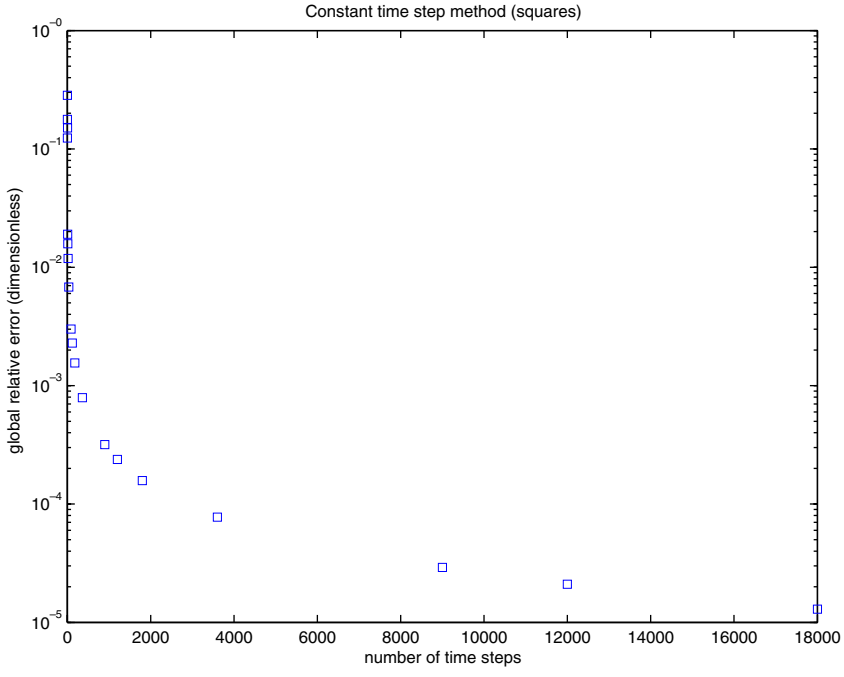

Fig. 12. Global relative error vs. number of time steps for the constant step size method.

which closely follows the physics of the problem. With the constant step size method, the relative error decreases from about .2 (for 1 time step) to 10^{-5} (for 18,000 time steps) (see Fig. 12). Similarly taking 14 time

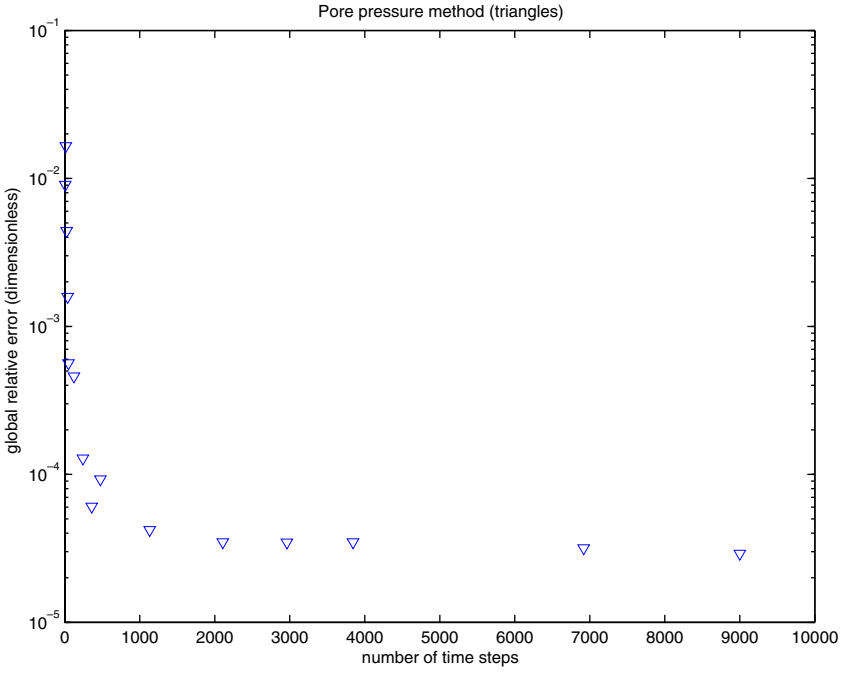

Fig. 13. Global relative error vs. number of time steps for the pore pressure method.

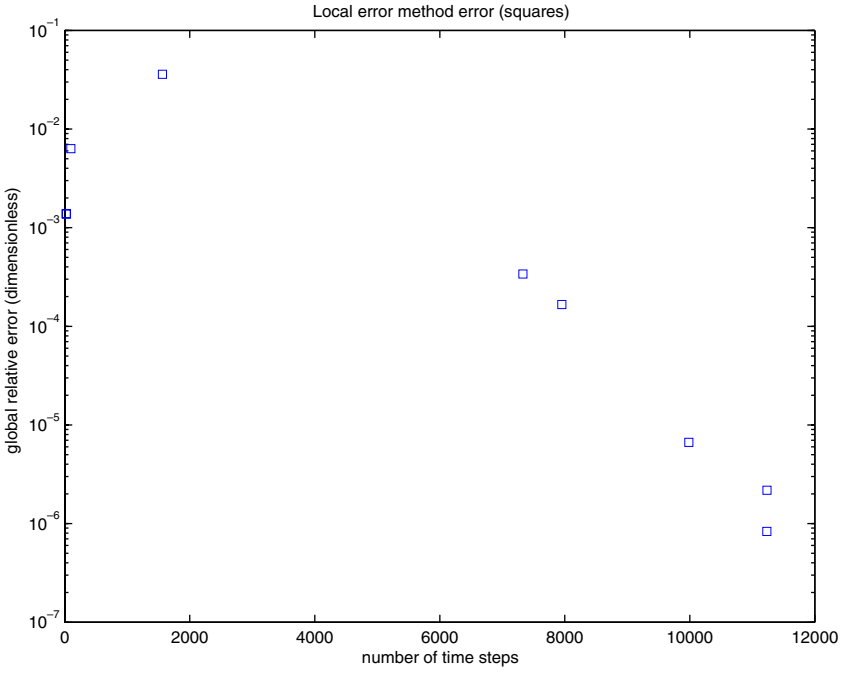

Fig. 14. Global relative error vs. number of time steps for the local error method.

steps of the pore pressure method resulted in a relative error of 1.5×10^{-2}. Taking 9000 time steps gave a relative error in the solution of 3×10^{-5} (see Fig. 13).

In contrast, the relative error from the local error method is not directly proportional to the number of time steps taken (Fig. 14). For some choices of goal local error tolerance, the relative error in the solution actually

increases as we take more time steps due to the quantization of the step size. Overall, however, we note that the local error method wins over the other methods in terms of error reduction. If one takes 11,000 steps of the local error method, the relative error is 8×10^{-7}. (Compare this minimum error with the error from the constant step size and pore pressure methods—10^{-5} and 3×10^{-5}, respectively.) The local error method is the most expensive method *per time step* as one first takes a step of size $2t$, and then resimulates the same time period using two steps each of length t. However, the change in step size is dramatic with this method and the large reduction in error indicates the accuracy of the adaptive time stepping scheme. Modifications can be made to the method to reduce the computational cost of repeating each step. For instance, one might choose only to retrace selected time steps (rather than every time step) to save computation. We have not tested such modifications of the local error method.

5. Conclusion

Accurate modeling of fluid flow in structurally weak reservoirs requires incorporation of realistic deformation physics. Such modeling can be extremely expensive, and a variety of avenues are available for reducing this cost. Loosely coupling together two independent simulators (one for flow and one for deformation) via an interface reduces the manpower needed to build the coupled code. However, the simulations themselves can still be computationally prohibitive to run. One major advantage of loose coupling is that the mechanics and flow solves need not occur at every time step. In fact, one may adaptively select the size of (and hence overall number of) time steps taken by examining the magnitude of change in output parameters.

The adaptivity in this work differs from that seen in most other examples because it is used in conjunction with a multiphysics simulator. The flow time step is in fact fixed, and the adaptive step size methods (local error and pore pressure) use output changes in displacement and pressure to determine how large of a mechanics step to take. Both methods appear to be very accurate for the Terzaghi test problem. The pore pressure method shows a linear dependence on tolerance (hence error reduction is directly correlated to time step size). It more closely mimics the constant step size method than does the local error method. The local error method is based on the Runge–Kutta–Fehlberg technique for speeding up the solution of ode's. It changes the time step size in quantized jumps and hence shows less of a correlation between solution error and tolerance (or step) size. The algorithm could be tuned to the physical problem which would likely result in a smoother time step size vs. error curve than is shown in this paper. It does appear, however, that the local error method outperforms the pore pressure method in terms of solution accuracy. While the constant step size and pore pressure methods reduced the relative error to 10^{-5}, the local error method produced results with an error of approximately 10^{-6}. The pore pressure method is the cheapest of the three methods (resulting in a solution with approximately the same accuracy as the constant step size method but in many fewer time steps). However, the local error method was the best able to drive down the total error. The local error method is the most expensive of the three methods in terms of cost per time step as each mechanics step is essentially taken twice, but improvements to this idea would be easy to implement. Ideally a heuristic for choosing the tolerance is needed. At the moment there is no clear way to optimize the time step even using adaptive techniques. Although an optimal mechanics step size was our initial goal, it is hard to imagine how to determine such a step without repeating the step (perhaps many times) thus losing the savings of adaptivity. Clearly, more work must be done on optimal time stepping for multiphysics simulations.

Acknowledgements

The authors thank Mike Stone of Sandia National Laboratories for his help with the mechanical deformation modeling and the Terzaghi validation problem. The second author gratefully acknowledges receiving support to perform this work under the UMBC Undergraduate Research Award Program during academic year 2002–2003.

References

[1] A. Yudovich, D. Morgan, Casing deformation in Ekofisk, J. Petr. Tech. (July) (1989) 729.

[2] J. Dangerfield, Ekofisk Field subsidence fault analysis using 3-D seismic, in: R.E. Sheriff (Ed.), Reservoir Geophysics, SEG, Tulsa, OK, 1992, pp. 110–121.
[3] J. Fredrich, J. Arguello, B. Thorne, W. Wawersik, G. Deitrick, E. de Rouffignac, L. Myer, M. Bruno, Three-dimensional geomechanical simulation of reservoir compaction and implications for well-failures in the Belridge Diatomite, in: Proceedings of the SPE Annual Technical Conference and Exhibition, No. 36698. SPE, 1996, pp. 195–210.
[4] M. Gutierrez, R. Lewis, I. Masters, Petroleum reservoir simulation coupling fluid flow and geomechanics, SPE Reservoir Evaluat. Eng. (June) (2001) 164–172.
[5] S. Minkoff, C. Stone, S. Bryant, M. Peszynska, M. Wheeler, Coupled fluid flow and geomechanical deformation modeling, J. Petroleum Sci. Eng. 38 (2003) 37–56.
[6] S. Minkoff, C. Stone, S. Bryant, M. Peszynska, Coupled geomechanics and flow simulation for time-lapse seismic modeling, Geophysics 69 (2004) 200–211.
[7] R. Lewis, Y. Sukirman, Finite element modelling of three-phase flow in deforming saturated oil reservoirs, Int. J. Num. Anal. Meth. Geomech. 17 (1993) 577–598.
[8] R. Lewis, Y. Sukirman, Finite element modelling for simulating the surface subsidence above a compacting hydrocarbon reservoir, Int. J. Num. Anal. Meth. Geomech. 18 (1993) 619–639.
[9] R. Lewis, H. Ghafouri, A novel finite element double porosity model for multiphase flow through deformable fractured porous media, Int. J. Num. Anal. Meth. Geomech. 21 (1997) 789–816.
[10] J. Osorio, H. Chen, L. Teufel, Numerical simulation of the impact of flow-induced geomechanical response on the productivity of stress-sensitive reservoirs, in: Proceedings of the 15th Reservoir Simulation Symposium, No. 51929, SPE, 1999, pp. 373–387.
[11] M. Gutierrez, R. Lewis, Coupling of fluid flow and deformation in underground formations, J. Eng. Mech. 128 (7) (2002) 779–787.
[12] A. Settari, F. Mourits, Coupling of geomechanics and reservoir simulation models, in: H. Siriwardane, M. Zaman (Eds.), Computer Methods and Advances in Geomechanics, Balkema, Rotterdam, 1994, pp. 2151–2158.
[13] R. Dean, X. Gai, C. Stone, S. Minkoff, A comparison of techniques for coupling porous flow and geomechanics, in: Proceedings of the 17th Reservoir Simulation Symposium, SPE 79709, Houston, TX, 2003.
[14] O. Sinkin, R. Holzlohner, J. Zweck, C. Menyuk, Optimization of the split-step fourier method in modeling optical fiber communications systems, J. Lightwave Technol. 21 (1) (2003) 61–68.
[15] R. Ewing, Problems arising in the modeling of processes for hydrocarbon recovery, in: R.E. Ewing (Ed.), The Mathematics of Reservoir Simulation, SIAM, Philadelphia, 1983, pp. 35–106.
[16] G. Middleton, P. Wilcock, Mechanics in Earth and Environmental Sciences, Cambridge University Press, Cambridge, 1994.
[17] M. Gockenbach, Partial Differential Equations: Analytical and Numerical Methods, SIAM, 2003.
[18] C. Gear, Numerical Initial Value Problems in Ordinary Differential Equations, Prentice-Hall, New Jersey, 1971.
[19] D. Kincaid, W. Cheney, Numerical Analysis: Mathematics of Scientific Computing, third ed., Brooks/Cole, Pacific Grove, CA, 2002.
[20] K. Terzaghi, R. Peck, Soil Mechanics in Engineering Practice, John Wiley & Sons, New York, 1948.
[21] Hibbitt, Karlsson, Sorenson, ABAQUS/Standard Example Problems Manual, Vol. 1, Version 5.8. Pawtucket, RI, 1998.
[22] H. Siriwardane, C. Desai, Two numerical schemes for nonlinear consolidation, Int. J. Num. Methods Eng. 17 (1981) 405–426.
[23] J. Wan, Stabilized finite element methods for coupled geomechanics and multiphase flow, Ph.D. thesis, Stanford University, Stanford, CA, 2003.
[24] A. Verruijt, Soil Mechanics. Delft University of Technology, http://geo.verruijt.net/, 2004.
[25] J. Carter, J. Booker, J. Small, The analysis of finite elasto-plastic consolidation, Int. J. Num. Anal. Meth. Geomech. 3 (1979) 107–129.
[26] R. Mitchell, Earth Struct. Eng., Allen & Unwin, Inc., Boston, 1983.
[27] R. Lewis, B. Schrefler, The Finite Element Method in the Deformation and Consolidation of Porous Media, John Wiley & Sons, New York, 1987.